Experimental Identification of the Behavior of Glass Fiber Bushing

Björn Nilsson

Department of Automatic Control **Lund Institute of Technology** **Box 118** **SE-221 00 Lund Sweden**	*Document name* MASTER THESIS
	Date of issue November 2000
	Document Number ISRN LTFD2/TFRT—5651--SE
Author(s) Björn Nilsson	*Supervisor* G. W. Chang, N. Marsault Veteotex International P. Hagander, T. Hägglund LTH.
	Sponsoring organization

Title and subtitle
Experimental Identification of the Behavior of Glass Fiber Bushing. (Modellering och reglering av glasfibertillverkning).

Abstract
Two different techniques exist for glass fiber production, direct melt bushing and marble bushing. The purpose of the project was to study the glass fiber production process and investigate the possibilty of constructing mathematical models from experimental data. This part also included implementation of a DAQ system to obtain the expeimental data. A second objective was to construct an efficent temperature control for a producion unit for glass fiber production.
The approach taken is to measure the electrical power supplied to the bushing and the glas temperature. From the I/O data a model in the form of a high-order transfer function for the process would be identified. With the model a controller which would minimize process variations would be constructed.
   The experiments shows that there is a large difference between the two techniques in terms of process disturbances. For the marble melt bushing only approximate models could be constructed. For the direct melt bushing the process disturbances was less important and models with small variances could be constructed.
 The approach taken would yeild stable, robust controller. However better control could propably be achieved if some measurable process disturbances like the glass temperature at the entry is incorperated. Another approach would be to use an adaptive controller. This approach would be best suited for the direct melt bushing with it's slowly varying process dynamics

Keywords

Classification system and/or index terms (if any)

Supplementary bibliographical information

Identification expérimentale du comportement d'une filiere
Experimental identification of the behavior of glas fiber bushing

Nilsson, Bjorn

November 1, 2000

Remerciements

Je tiens à exprimer, par ces quelques lignes, mes plus vifs remerciements à mes encadreurs de projet, Gi-Won Chang et Nicolas Marsault. Qu'ils soient assuré de ma sincére reconnaissance pour la confiance qu'ils m'ont témoigné.

Je tiens à remercier Bruno Gibello et Louis Lugaz, qui se sont chargés de faire les essais dans la passerelle et Emmanuel Vaquant et Frédéric Vernet pour leurs collaborations.

Je remercie spécialement les gens de Laboratoire d'Automatique de Grenoble, LAG, INPG, M. Luc Dugard, M. Paolino Tona et M. Olivier Sename qui m'ont beaucoup aidé avec la partie théoritique pendant ce stage.

Avant de finir je veux aussi remercier tous les gens que j'ai rencontrés pendant ce stage pour leur soutien. Specialment je voudrais remercier les deux personnes avec qui j'ai partagé le bureau, Cecile et Jean-Christophe pour leur générosité et gentillesse.

Contents

List of Figures

List of Tables

Chapter 1

Introduction

1.1 English

In glass fiber production the temperature control plays an important role for the quality of the produced glass fiber. The purpose of a stable temperature is two-fold. As the viscosity of glas is strongly temperature depending at the temperature ranges in the bushing and as the glas outflow in turn depends on the viscosity, the glass flow is related to the temperature in the bushing. A stable temperature will then give less variations in the fiber thickness. In addition a more stable environment is likely to give fewer production breaks. To construct a powerful controller it is necessary to have a mathematical model of the system to be controlled. This model can be obtained in a variety of ways. Sometimes it is possible to obtain good models from modeling alone, that is to build the model from physical laws, but if the system is more complex an experimental identification should be useful. Normally one uses a combination of the two, a priori knowledge for the experiment design and perhaps for the choice of model structure, and then the experimental data is used to find the coefficients of the model. The glass fiber bushing contains many difficulties. It is both non-linear and time-varying. Care has to be taken in order to obtain robust models.

1.2 Français

Pour le procédé de fabrication de fibre de verre la réglulation de temperature joue un rôle important. Il y a deux objectives principaux. Le premiér est que

la debit de verre est fortement liée à la témperature. Une témperature stable diminue donc les variations d'épaisseur pour les fibres. Le deuxième est qu'une témperature stable donne des flux plus calmes et stables ce qui très probablement va diminuer le nombre de cassés. Pour obtenir une régulation efficace il est nécessaire d'avoir un modèle mathématique du le systéme. Ce modéle peut être déduit soit à partir de la connaissance des equations physiques qui gérent le système soit à partir d'une identification basée sur des données expérimentales. Le procedé de fabrication de fibre de verres est une procédé très difficile a modéliser. Il a une comportement variant dans le temps et aussi non-linéaire.

Chapter 2

Presentation of the project and its context

The project is carried out in two locations

2.1 Initial conditions

At the start of this project models for the direct melt bushing based on numerical simulations existed at VI. The bushing is treated as a single input single output system, where an electrical power is used to control the temperature. The temperature control is made by numerical controllers based on a PID control. In the Verrerie this control originates from the 70's whereas for the Passerelle the equipment is newer.

2.2 Objective of the project

The goal of this project was to continue the studies of the temperature control of the glas fiber bushing process. Our approach would be to make experiments and try to calculate a model from the experimental data. A subgoal of the project was thus to obtain models for the bushing.

Chapter 3

Theoretical studies

In this chapter I will discuss the theory in this project. I will start with an analysis of the bushing physics and continue by discussing some general theory of identification.

3.1 The Glass fiber bushing

During the first week a theoretical study of the physics of the bushing process was carried out. This study served to give an estimate of what time coefficients and which gains to expect.

There exist two glass fiber bushing techniques, direct melt bushing, see figure B for a schema, and marble bushing. The difference resides in the way the glas enters the bushing. For the direct melt bushing the glas is preheated to liquid form and enters the bushing in liquid form and at a high temperature. For marble bushing glas balls are supplied to the top and enters the bushing through small holes. Thus the glas is transformed to liquid form first when it enters the bushing. Both techniques use a perforated base plate to produce the glas fiber. In terms of operating stability and general performance the direct melt bushing technique is preferable to the marble bushing. The brutal jump in temperature when the glas enters the bushing is avoided and more stable flows should be obtained when the glass enters in liquid form. For a more exhaustive description of the bushing I refer to existing literature and earlier works.

3.1.1 The bushing physics

I will start my discussion of the bushing physics with the description of the change in thermal energy of an object

$$\Delta Q = m * c_p * \Delta T \tag{3.1}$$

where Q denotes energy, m mass, c_p the specific heat capacity and T is temperature. The change of energy for a system is equal to

Change in Energy per time unit = energy flow through the boundaries + energy sources or sinks.

Or mathematically

$$\frac{\Delta Q}{\Delta t} = S + \phi_{in} - \phi_{out} \tag{3.2}$$

Where ϕ_{in} denotes inflow, ϕ_{out} the outflow and S the sources.

A complete analysis of all the details of the thermal exchanges is very complex, however a quick study should still be useful. The part of the process that I'm considering is the part of the process in figure A.2. I will assume that all variables are kept constant, glass mass, supplied power etc, except for the temperature. To determine the temperature in the bushing we need to know the energy flows as well as the energy sources and I have listed them in table 3.1.

- Convection, mass transport in form of glass that enters and leaves the bushing as well as redistribution of the energy within the bushing.

- Thermal Conduction, energy flows from the platin-rodhium shell heated by electrical power to the glas and towards the outside

- Radiation. As glass is a semitransparent material energy radiated from the platin-rodhium shell is absorbed throughout the glas mass. Energy is as well radiated to the surroundings.

- All energy to the system is supplied by the electrical power

Table 3.1: Energy flows and sources in the bushing

At the output the glass is quickly cooled thanks to cooling fins. Here energy is lost both by radiation, conduction and convection. The conduction part corresponds to $\phi_{cond} = hA(T_{glass} - T_{fins})$ where h is the thermal exchange coefficient and A the interface area whereas the radiation part is $\phi_{rad} = Ae\sigma T_{glass}^4$. The convection part corresponds to $\phi_{convout} = \dot{m}c_P T$. The glass that enter at the top gives the flow $\phi_{convin} = \dot{m}c_P T_{in}$. The only energy source is the electrical power. The two massflows $\dot{m}$ must be equal if the mass in the bushing is to be constant. Inserting these relationships in equation 3.2 and letting Δt approach zero yields

$$\frac{\delta(mc_p T_{glass})}{\delta t} = P - hA(T_{glass} - T_{fins}) - Ae\sigma T_{glass}^4 + \dot{m}c_P T_{in} - \dot{m}c_P T_{glass}$$
$$(3.3)$$

Neglecting the radiation part of this equation and rearranging finally gives equation 3.4.

$$\frac{\delta(mc_p T_{glass})}{\delta t} + T_{glass}(\dot{m}c_P + hA) = P + hAT_{fins} + \dot{m}c_P T_{in} \qquad (3.4)$$

this becomes an ordinary first order differential equation with the solution

$$T = staticlevel + C_1 e^{-\frac{t(\dot{m}c_P + hA)}{m * c_p}} \qquad (3.5)$$

From equation 3.5 the time constant,τ, for the bushing is equal to

$$\tau = \frac{m * c_p}{\dot{m}c_P + hA} \qquad (3.6)$$

A check of physical units give that τ will be expressed in seconds when using SI-units.

Three conclusions can be made from this discussion. The relation between power and temperature is certainly nonlinear. As the approximations made arriving at equation 3.6 is rather large an estimate using this formula could be rather far off target. It should however portray the relationship between the variables and the time constant, such as an increase in mass will increase the time constant. In addition the relation between power and temperature is time varying. It is not a very likely assumption that neither the massflow nor the thermal exchange coefficient at the bottom nor the glassmass in the bushing changes. If these parameters change the relation between temperature and power will also change.

11

3.1.2 The glas fiber bushing used during this project

During this project we have worked with several different types of bushing. Experiments on both types of bushing have been made. In addition the size of the bushing has varied. From the larger bushing in the production to smaller lab versions.

3.1.3 Earlier work

Studies to find a mathematical model for the behavior of the bushing has been carried out. These studies have been aimed at constructing a simulation program based on the physical equations that govern the process. This program have then been used to simulate step responses from which first order models have been identified. The development of this solver has been focused on simulations of direct melt bushing since it is the most common type. These models use the tension over the bushing as input. However, as the temperature is rather proportional to the power, and thus the square of the tension, it would be more informative to express the gain with power as the input. Equation 3.7 shows the relationship between $\frac{\Delta P}{P_0}$ and $\frac{\Delta U}{U_0}$

$$\frac{\Delta P}{P_0} = \frac{(2U_0 \Delta U + (\Delta U)^2)/R}{(U_0)^2/R} = 2\frac{\Delta U}{U_0} + \left(\frac{\Delta U}{U_0}\right)^2 \qquad (3.7)$$

3.2 Estimation of gains and time constants

It is good practice to start an identification by determining which gains and time constants to expect. As shown in the previous section a relationship should be sought between the power and temperature, and in this section I will try to estimate the static gain and the rise time for a unit step in power.

For a first order transfer function, equation 3.8, the static gain corresponds to K_p and the time constant to τ.

$$\frac{K_p}{1 + \tau s} \qquad (3.8)$$

From my previous discussion in section 3.1.1 an approximation of τ was derived in equation 3.6. In table B.3 estimations of the coefficients is given for a bushing unit of type 2241US. These values gives $\tau = 33$s.

In the report by N. Zaher an estimation is made of the properties for bushing 2241US. Values for the power was supplied by Samuel Viboud and those for the temperature were taken from the report, annexe 13. The rise time should not be affected and the values are taken directly from the report, page 53. The gain and rise time are presented in table 3.2 and the values used can be found in table C.1

Gain (° C/kW)	Gain (%/%)	Rise Time (s)
16.99	0.27	441

Table 3.2: Temperature/Power rise time and gain for bushing 2241US

As no simulations exists for the smaller bushing used during this stage, I will instead try to make a qualitative statement about their behavior relative to the larger simulation ones. In view of equation 3.6 smaller bushings should have shorter rise times. As for the gain, the temperature depends on the thermal energy per mass unit. This fact makes it probable that the gain is greater for smaller bushings because an increase in energy is divided on less mass.

3.3   A priori disturbance models

Earlier studies have shown that the disturbances mainly originates from two sources. Variations in the thermal exchange coefficient at the bottom of the bushing and variations in the glass mass in the bushing, or equivalently the height of glass in the bushing. Little is known about the influence of these disturbances on the bushing. Simulations has been made and first order transfer functions has been identified. However no measurements have been made on the variations in height and exchange coefficient. From the simulations made the process seems to be equally sensitive to changes in height and thermal coefficient as the tension. Thus an effort should be made to reduce variations to a minimum during experiments. Once again a qualitative statement can be made for the smaller bushings. These should be more sensitive than the larger ones and stable conditions is even more important.

3.4 The identification process

The goal of an identification is to find a mathematical model that describes the dynamical behavior of a system. Two ways exist for creating a model, derive it from knowledge of the rules that govern the process, or use experimental data to create it. In this section I will discuss general theory for creating models from measured data. As for any operators used in this discussion I have adopted the same conventions as in Ljung.

3.4.1 Building a model from measured data

A model is built from three basic blocks. The building stones are

Input-output data
Model set
Criteria to choose the best model

The process of obtaining these blocks is described by the schema from the book of Ljung, in figure 3.1. At the end of the chain a validation of the model is carried out. If the result shows that the obtained model doesn't sufficiently describe the system, then an analysis of the result has to be carried out to modify some part of the chain. As the chain is repeated the knowledge of the system increases and so the quality of the model.

Experiment design

In this step an input sequence is decided. This sequence should be as informative as possible, i.e. have a strong frequency content in interesting frequency ranges. This is important in view of equation 3.14, as it states that the stronger the power in a frequency range the better the estimated model is for that frequency. This step also includes choice of measurements, choice of DAQ system and how to setup up this system so as to minimize measurement noise. This step is very important, without good data it is harder and requiers more work to obtain useful models, and the quality of the final model will suffer.
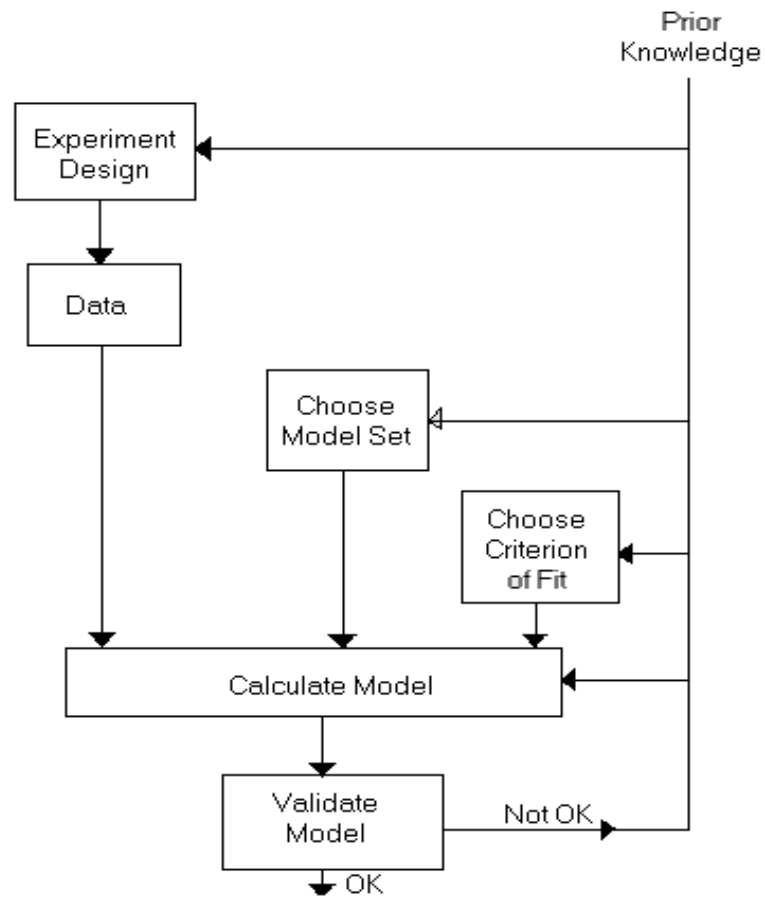
Figure 3.1: The system identification procedure

Choice of model structure

If there exist some sort of a priori model structure from a modeling of the process this is of course the natural choice. If one is not so lucky as to have an a priori structure one should consider what to expect. If there is a strong influence on the system from disturbances, this would require that a model structure that allows modeling of these disturbances is chosen. It could also be useful to consider if there exist some good parametric adaptation algorithm to use.

Model order

If the system is nonlinear the goal is to find a linear system that approximates it around a certain point. In terms of simulating a higher order would produce a better result. The downside of a higher order model is however that it becomes more complex to construct a controller. For first or second order model there exist several easy to use tuning rules for PID controllers for example. Thus if the difference in fit between a high order and a low order model the lower could still be chosen.

The linear model

The standard way to describe a linear model is by equation 3.9.

$$y(t) = G(q) * u(t) + v(t) \tag{3.9}$$

Any disturbance v(t) can be realised by a filtered white noise e(t). that is it is an independent random variable with zero mean and variance λ

$$v(t) = H(q) * e(t) \tag{3.10}$$

With equations 3.9 and 3.10 a linear system is completely described by $G(q) = \sum_{k=1}^{\infty} g(k)q^{-k}$ and $H(q) = \sum_{k=1}^{\infty} h(k)q^{-k}$ and λ. To describe a models parameter dependence θ is used.

In appendix D the most common models are listed.

Choice of sampling interval

When creating a discrete controller for a system the choice of sampling period is important. There exists several rule of thumbhs on how to choose the

sampling period. One is to choose the sampling time so that relation 3.11 holds, where τ is the rise time and $T_{sampling}$ is the sampling time.

$$\tau/4 < T_{sampling} < \tau \tag{3.11}$$

It could be interesting to use this sampling period during both the acqusition of data and the construction of a model so that the correct sampling time is directly obtained.

3.4.2 Algorithmes

The discrete nature of the measured data and of computers make it natural to work with discret models during an identification. It exists powerful estimation algorithms for discret models, whereas no such methods exists for higher order models in the continuous case. The discret algorithms also allow a greater flexibility on the I/O data. These discret models can afterwards be converted into continuous time ones if desired.

Prediction error methods

A common type of methods are Prediction Error Methods(pem). The basic idea is to make a prediction of the output and then to change the parameters in the model so that the difference between prediction and measurement is minimized. Typically the whole data set is first acquired and then a prediction is calculated for each instant. The model is then chosen so that the sum of all predictions are minimized. Normally one minimise a function $l(\epsilon, t, \theta)$ of the difference. A common choice is the square of the error. This is known as the least square(LS) identification. Mathematically this is described by choosing the parameters in θ_N so that the cost function $V_N(\theta, Z^N)$ is minimized, with

$$\hat{\theta}_N = argmin_{\theta \in D_M} V_N(\theta, Z^N) \tag{3.12}$$

$$V_N(\theta, Z^N) = \frac{1}{N} \sum [l(\epsilon(t, \theta), \theta, t)] \tag{3.13}$$

17

Model properties

The error between the real model and the estimated one can be decomposed in two parts, a biais and a variance. The biais is the error between the estimation as N goes to infinity $G^*(q)$ and the real system. The variance describes how quickly the identified model converges to this limit. In chapter 8, theorem 8.4, in the book of Ljung a theorem for the biais of a pem is given. If the number of data, N, approaches infinity the estimate $\hat{G}(e^{iw}, \theta_N)$ will converge towards the real system $G_0(e^{iw})$ under the condition that the true model exists in the model set and the input is informative enough.

As for the variance the following equation is given in the same book, chapter 9

$$Cov\hat{G}_N(\theta, e^{iw}) \sim \frac{n}{N} \frac{\Phi_v(w)}{\Phi_u(w)} \tag{3.14}$$

A quick analysis of this expression gives that the model variance is large for large disturbances, and small for large inputs. The variance also decreases as the number of data increases ans increases as the order increases.

3.4.3 Validation

There exists several ways to validate a model and any assumptions made. It is wise to use several validation methods and not just look at one. Normally one has several different models to validate and one choose the one that gives the best results, keeping in mind the previous discussion about model complexity.

Fit between simulated and measured output

A good start is to make a simulation and compare the output with measured data. If the fit is good then the model is likely to describe the system well. Taking the least square error gives a numerical value for the fit. The smallest fit is however not necessarily the best model. The way the model captures the dynamics have to be taken into account.

Fit between predicted and measured output

If there are strong disturbances these might draw away the measured data from the simulated data and give a bad comparison even if the model between

input/output is good. In this case one might try to make a prediction of the output and look at the fit between prediction and measurement.

Residuals

Yet another method is to calculate the correlation between the error and input. If there is a strong correlation between the two something is missing in the model, as the disturbances are supposed to be independent of the input. In addition the error is assumed to be a white noise. Calculating the autocorrelation for the error thus gives an idea about the quality of the model.

Comparison with a priori modeling

A comparison with a priori model can be made to determine the quality of the model.

3.4.4 Closed loop identification

In some cases it might be necessary to stay in closed loop. This might be the case when the system that is to be identified is used for production and a production stop would cost a lot of money.

Direct identification

Consists of carrying out an identification between the input and the output using the algorithms from the open-loop case. For a pem the estimated model will still converge towards the real system under the same assumptions as in the open loop case.

3 step method

The three step method consist of the following steps.

Here u_r and y_r denote the reconstructed signals. In these signals the effect of any noise and perturbations have been removed. If the sensitivity functions are modeled sufficiently well this will result in a non biaised estimation according to chapter 5 in J. Chebassier.

- Determine the complementary sensitivity function.

- Determine the sensitivity function on the input

- Reconstruct u_r and y_r with r and the above functions

- Identify the model from u_r and y_r

Table 3.3: The three step method

Closed loop validation

If one has closed loop data the model should be validated in closed-loop simulation. That is the control loop is simulated and the reference is used to simulate the output. This requiers knowledge of the controller transfer function.

Chapter 4

Equipment and experimental setup

In this section I will discuss the various equipment and computer programs used during this project. I will start by presenting the mathematical tool Matlab, continue by describing our measuring equipment and finally discuss the measurement chains and the experimental setup in the Passerelle and the Verrerie.

4.1 Matlab and the Identification Toolbox

Matlab is a mathematical tool for making calculations. It is constructed so as to handle matrix operation quickly. From a control point of view there exists several useful toolboxes for making calculations with and examining properties of dynamical systems. A short list of Matlab features useful in an automation domain.

- Transfer function calculations

- Allows examination of dynamical system properties, through bodeplots, nyquist plots etc.

- Prewritten functions for constructing controllers from a dynamical model

In the identification toolbox are the algorithms discussed in the theory section implemented. It exists a Graphical User Interface(GUI) for this toolbox, were data can be treated easily and the different estimation methods,

model structures and pretreatment choices are easily accessible from drop down menus. The GUI also allows to examine different properties of the identified model and can advantageously be used to validate obtained models. The identification toolbox and the GUI contain the following functions

- Implementation of the algorithms in section 4.2.1

- Allows comparison of simulated output and measured output as well as residual properties for the simulation

- Visualisons of model properties, such as step responses, noise levels, poles/zeros and frequency content.

4.2 Measuring equipment

FP-1000, FP-AI-110, FP-TC-120, FP-AO-200, Computer with Labview and Fieldpoint Explorer

4.2.1 FieldPoint

FP is a distributed I/O system with high resolution and low noise levels. It contains numeric and analog I/O modules and network modules. A FP system consist of at least one network module with one or several I/O modules connected. The network module serves to communicate between the I/O modules and an ordinary computer.

4.2.2 Labview

Labview is program that can communicate with FP network modules, and it is useful for visualisation and data treatment. A Labview program is written in a graphic programming language called G+, which is rather user friendly.

4.3 Passerelle

The passerelle is a laboratory where three bushings of the type marble bushing is used for experimatal purposes. Here our first experiments were made. I will start by describing the glass fiber bushings, continue with the existing control equipment and finish by describing our experimental setup.

4.3.1 The glass fiber bushing

Three different bushing was used for the experiments in the passerelle, numbered one, two and three. All of them is of type fusion billes. The differences between the three lies in the number of holes, the existence of a cabine or not, and if there existed some sort of control for the flow of glass balls. Se table 4.1

Number	Code	Number of holes	Cabine	Control of balls
1	BEC-274-185	400	No	No
2	FB08-1152	800	No	No
3	FB08-1175	800	Yes	Yes

Table 4.1: Bushing in the Passerelle

4.3.2 Measuring and control equipment

Siemens PLC S5-95U, Voltage/Current transformateurs, Bushing, Thyristor, Thermocouple, Supervision computer

To measure the temperature a thermocouple of type B is welded on one side of the bushing. The tension output from the thermocouple is linearized and transformed to a current of 0-20 mA. This current pass a numerical display before arriving at the PLC. The display measures tension in the interval 0-10V so a resistance of 500Ω is put over the input. In the PLC the temperature is calculated as $T = U * \frac{1600}{10}$ where U is the measured tension in Volts. The PLC calculates a command current which controls a thyristor that control the power in the bushing. The relationship between control current and power is linear. Se figure E.1 for a schema.

4.3.3 Experimental setup

We choose to measure the input voltage of the S5-95U, the output current from the S5-95U as well as the effective current and tension in the bushing. In addition the reference signal for the temperature was saved with Labview. Our experimental setup is depicted in figure E.1.

The Labview Fieldpoint controller

The same control equation as in the S5-95U was implemented, see equation E.4. In table 4.2 the coefficients used for the control are given.

TI	K_d
0.8	3

Table 4.2: Values used for the control with Labview

4.4 Verrerie

The Verrerie is a glass fiber production plant where only direct melt bushing is used. In this part I start with describing the bushing used, continue with the control equipment and finish with our experiimental setup.

4.4.1 The glas fiber bushing

Our experiments was made on a bushing of type 2241US, and thus of type direct melt. For the characteristics of this bushing se annexe B. Our measurements was made in avant-corps 7, on bushing 75.

4.4.2 Measuring and control equipment

A thermocouple of type B welded on one side of the bushing measures the temperature. The command signal is a current that controls a thyristor which in turn control the power in the bushing. The power from the thyristor pass a transformer which in turn supply the bushing with power. Before the transformer the power is called primary and after secondary power. Two bars go from the transform to each side of the bushing respectivly. These bars serve to supply the electrical power. The control is made by a TCS-6352 that communicates with a supervision computer.

4.4.3 Experimental setup

The secondary power for the bushing was measured with Fieldpoint. Clamps were connected to the bars to measure the tension. Because of the strong

current an indirect method had to be used to measure it. The method used consisted of placing a cable around the bar that supply the electrical current to the bushing and measure the induced current. The values in the TCS was recuperated with Intouch. Our experimental setup is depicted in figure F.1.

Chapter 5

Identification and measurements

In this chapter I will discuss the various measurements made, Measurments were made in two different locations, the Passerelle which is a lab, and at the Verrerie, which is a factory used for glass fiber production. I will start by describing the measuremnts in the Passerelle and finish with the measurments made in the Verrerie.

5.1 The identification and measurements in the Passerelle

This lab contains three bushing which is used for experimental purposes. Because of this we enjoyed a large degree of freedom in experiment design here, as opposed to the experiments in the Verrerie where we were constrained due to the fact that production quotas has to be met.

5.1.1 Experiments

Several measurement series were made in the passerelle. We started out by trying the most straightforward methods and moving on towards more advanced methods. Below I have described in chronological order the experiments made and improvements made over the course of the project.

Choice of sampling period

Using the value from the simulation and the rule of thumb in relation 3.11 would indicate a sampling period of around 100s for the larger 2241US bushing. We decided however to sample every second and leave the choice of sampling period to after the data was obtained.

Initial experiments

The initial series was made on bushing 2. The first series was made with the objective to obtain open-loop step responses. The result is shown in figure 5.1. As the effect of the current step is completely hidden by perturbations this data isn't useful for an identification. A second open-loop experiment were made with a PRBS sequence as input but the result was equally bad.
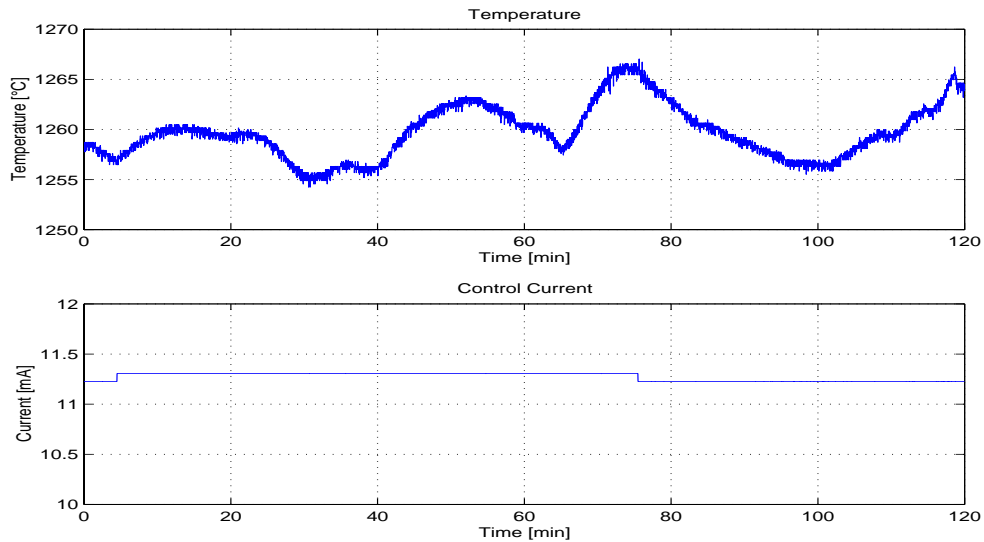

Figure 5.1: Open loop data from bushing two in the Passerelle

Closed-Loop experiments

As we didn't have the possibility to change the bushing at this point we decided to make closed-loop measurements. The identification becomes more difficult with closed-loop data but it is still possible to obtain good models. As the experiments at the Verrerie had to be made in closed-loop this had the additional advantage of testing the methodology for constructing models from closed loop data. The measurements obtained during closed-loop still contained strong disturbances and the identification gave poor results in terms of capability of reproducing the measured output. At this point we obtained the means to access the data 'inside' the S5-95U, and it was decided to make a new series to verify the performance of the S5-95U.
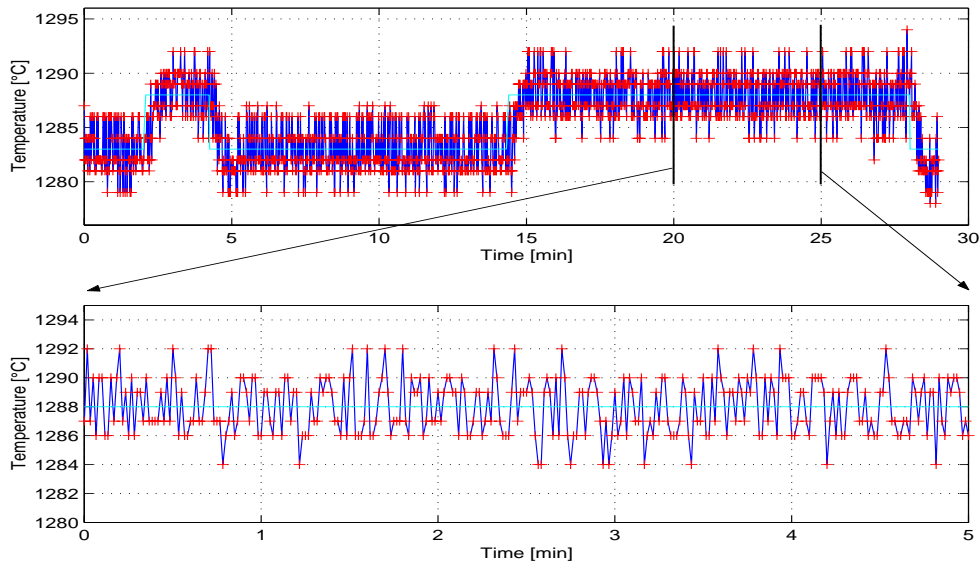
Figure 5.2: Temperature within the S5-95U

The result from these experiments, see figure 5.2 showed that the measurement noise in the controller was significant ($\pm 4°$C). As the moving average of the input noise is slowly varying this data introduced a slowly varying action which in turn generated a slowly varying temperature. Such behavior is not preferable. Because of the poor performance of the S5-95U a study was carried out in order to improve the control performance to obtain better identification data. Two possibilities was considered. Either the S5-95U was

28

to be reprogrammed or the control was implemented with Labview and FP. The comparison is made in appendix K. This analysis showed that better results could be obtain using Labview and Fieldpoint. Since the DAQ part of the controller was already written it was also quick to implement the new controller. It was thus decided to make new measurement series to obtain the highly desirable identification data.

The final series

Theses experiments was made on both bushing 2 and 3. After an initial test of the new control system on a smaller bushing plant it was installed parallel to the S5-95U. This made it possible to switch back to the S5-95U regulation quickly if something did not work, in order to protect the bushing plant. With the new controller a new set of measurements was carried out.

5.1.2   The identification

A data treatment was carried out after each experiment with the ambition to obtain a good model for the bushing. It was not until the last measurement series that models which gave reasonably good validation results could be obtained.

Throughout the identification process I've worked with Matlab and in particular with the identification toolbox. Examples of command sequences used to obtain models are given as .m matlab files in annexe H.

Choice of model structure

Given the complex behavior of the bushing process and the fact that it is both non-linear and time varying a complex structure would be needed. However the properties of the identification algorithms is such that for a simpler structure the estimated model will converge quicker towards the limit. Thus all different model structures available have been tested. The exception is state space models for which the algorithm doesn't work with closed loop data.

Calculation of models

The data which gave the best results was the data obtained from bushing 3. One data set was chosen as working data, FP3, and another for valida-

tion, FP1, see figure I.1 for plots. The data was prefiltered to reduce the influence of measurement noise before use with the identification algorithms. A prediction error method was used to calculate the parameters for a given model.

Choice of best model

To choose the best model I primarily looked at two things. The fit between simulation and measurement and the correlation between input and output.

Closed-loop Validation

A final validation of the models was made by a simulation in closed loop. In figure J.6 the result of this simulation is plotted. The simulation has been made both with the identified third order model and a first order approximation based on this model.

5.2 The identification and measurements in the Verrerie

In this section I will start by discussing the measurements made at the Verrerie and continue with the identification from the obtained results.

Our experiments here were made on a bushing plant in production. As production breaks was rather costly extra care was taken in designing the experiment to avoid this.

5.2.1 Measurements

Three series was made in the Verrerie. The two best ones were chosen as work data and validation data. See figure J.2 for measured temperature and reference signal.

5.2.2 The identification

The same decisions as in the passerelle were made, see section 5.1.2 for details.

Chapter 6

Results

6.1 Passerelle

Resulting models

See annexe I for graphs of the fit and residual. The static gain and an approximate time constant for a first order model for the bushing are given in table 6.1 from the model obtained by Direct Identification. The percentage gains has been calculated with the averages of FP3. In table I.1 average values for supplied power, control current and temperature with reference signal and change in reference are listed.

	Gain	Gain (%/%)	Time constant(s)
Command	9.5 (° C/mA)	0.11	134
Power	6.7 (° C/kW)	0.10	120

Table 6.1: Time constant and gain for bushing FB-08-1175

Errors

During the final series we changed measuring location for the input tension. Here we discovered that there is a fall in tension of about 2.5% from the display. Assuming that the tension over the display corresponds to the temperature this would make the gain 2.5% to low. As for the model uncertainty

a 99% confidence interval is plotted with the step response in fig I.4, and the standard deviations of the coefficients are given in table I.2.

6.2   Verrerie

Resulting models

See annexe J for graphs of the fit and residual. The static gain and an approximate time constant for a first order model for the bushing are given in table 6.2 from the model obtained by the three step method. The percentage gains has been calculated with the means from Verr3. In table J.1 average values for supplied power, control current and temperature with reference signal and change in reference are listed.

	Gain	Gain (%/%)	Time constant (s)
Command	3.3 (° C/OP)	0.21	85
Primary Power	7.7 (° C/kW)	0.18	89
Secondary Power	10.1 (° C/kW)	0.18	89

Table 6.2: Time constant and gain for bushing 2241US

As the temperature and secondary power were saved on two different computers the values are not synchronized and an identification with the secondary power was not possible. The values given in table 6.2 is calculated by equation 6.1. The rise time are the same as for the primary power.

$$\frac{\Delta T}{\Delta Ps} = \frac{\Delta T}{\Delta Pp}\frac{\Delta Pp}{\Delta Ps} \tag{6.1}$$

For closed-loop simulation shows that the models are not very good. Their rise time is to quick. This would probably be due to the poor precision on the measured temperature.

Error

Our tension was measured before the terminal clamps. As the connection between the clamps and the bushing isn't perfect, there might be a small air gap this will introduce a small fall in tension. Thus the power supplied to

the bushing should be smaller than our values and the gain is larger. Also, Intouch only allowed us to register the temperature as integers. This does introduce a large uncertainty in our model. In fact, the effect of rounding of the measure to integers will give the error $\frac{2}{6} = 33\%$ for the static gain, as the step in output is only 6° C.

6.3 Conclusion and Discussion

As for the marble bushing the conclusion have to be that the system dynamics are strongly time varying. As the glass enters in solid form this technique does not seem to allow sufficiently stable flows to keep a constant glass mass in the bushing. The obtained value for the gain could perhaps be seen as a time average. For the direct melt bushing the conditions were more stable, or at least more slowly varying, and the fit is also better for the simulation. With a longer sequence and more precision in the temperature measurement a better model can be obtained.

Chapter 7

General perspective and conclusions

A measuring system was created with Labview and Fieldpoint. This configuration combines a high quality data acquisition part with an easy to use and powerful programming language. This system was then expanded and made able to control a bushing in the Passerelle .

Several measurements series were made to investigate the physical properties of the bushing. The relation of main interest was between supplied electrical power and the temperature. Mathematical models for this relation was calculated from experimental data for two different kind of bushing. These models were then compared to models obtained from heavy numerical simulations. The static gain for both simulation model and experimental was roughly the same, however the simulation model had a much longer rise time than the experimental models.

In addition to these models the control parameters in the Passerelle was fine tuned to obtain better set point following and disturbance rejection.

Our experiments showed that improvements can be made on both the control and the acquisition part in the Passerelle. It is also my opinion that better control can be accomplished, both in the Passerelle and the Verrerie, if more measurements are included when controlling the temperature.

Appendix A

The glass fiber production process

In figure B is a schema over the direct melt bushing technique. With the direct melt bushing technique the glass mass (verre) is heated to liquid form in an oven (four). The glass are then transported in channels (canal) to the bushings (filière). The bottom plate of the bushing is perforated to allow for the glass to flow out as strands. An electrical power is supplied to the bushing in order to achieve the correct glass temperature. In figure A.2 is the part for which the energy calculations is made.
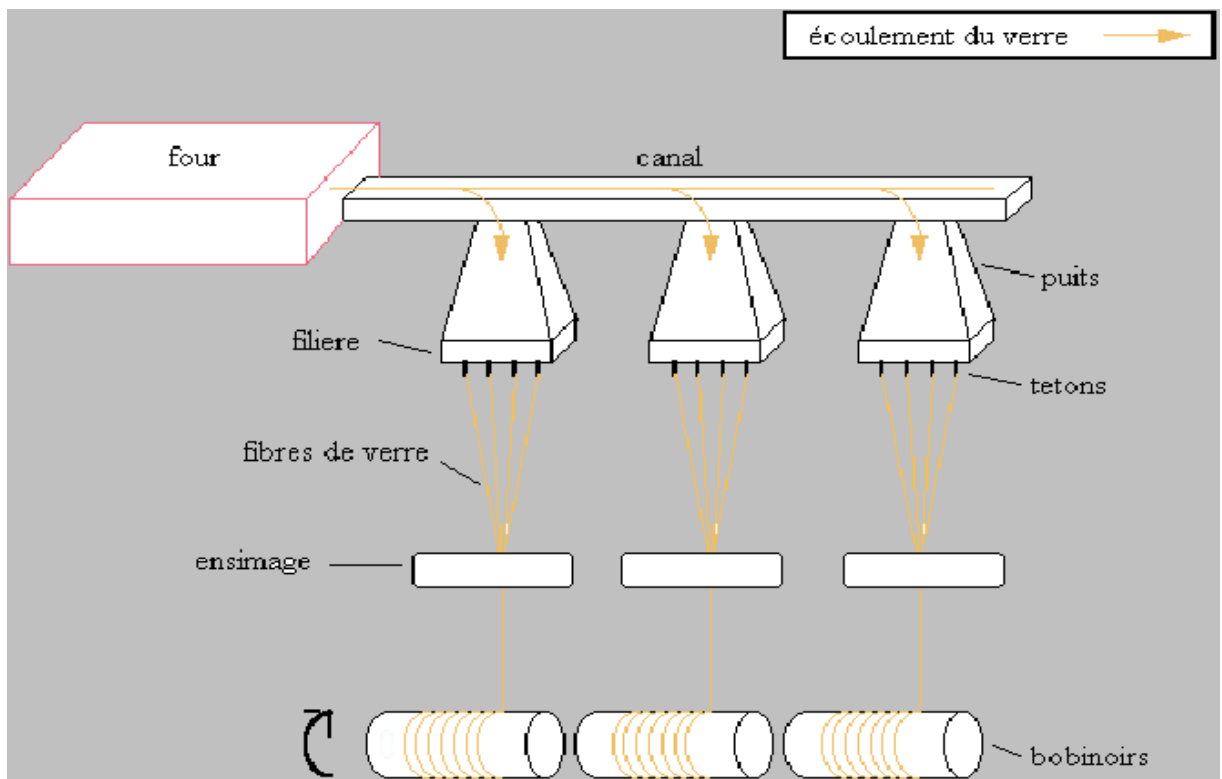
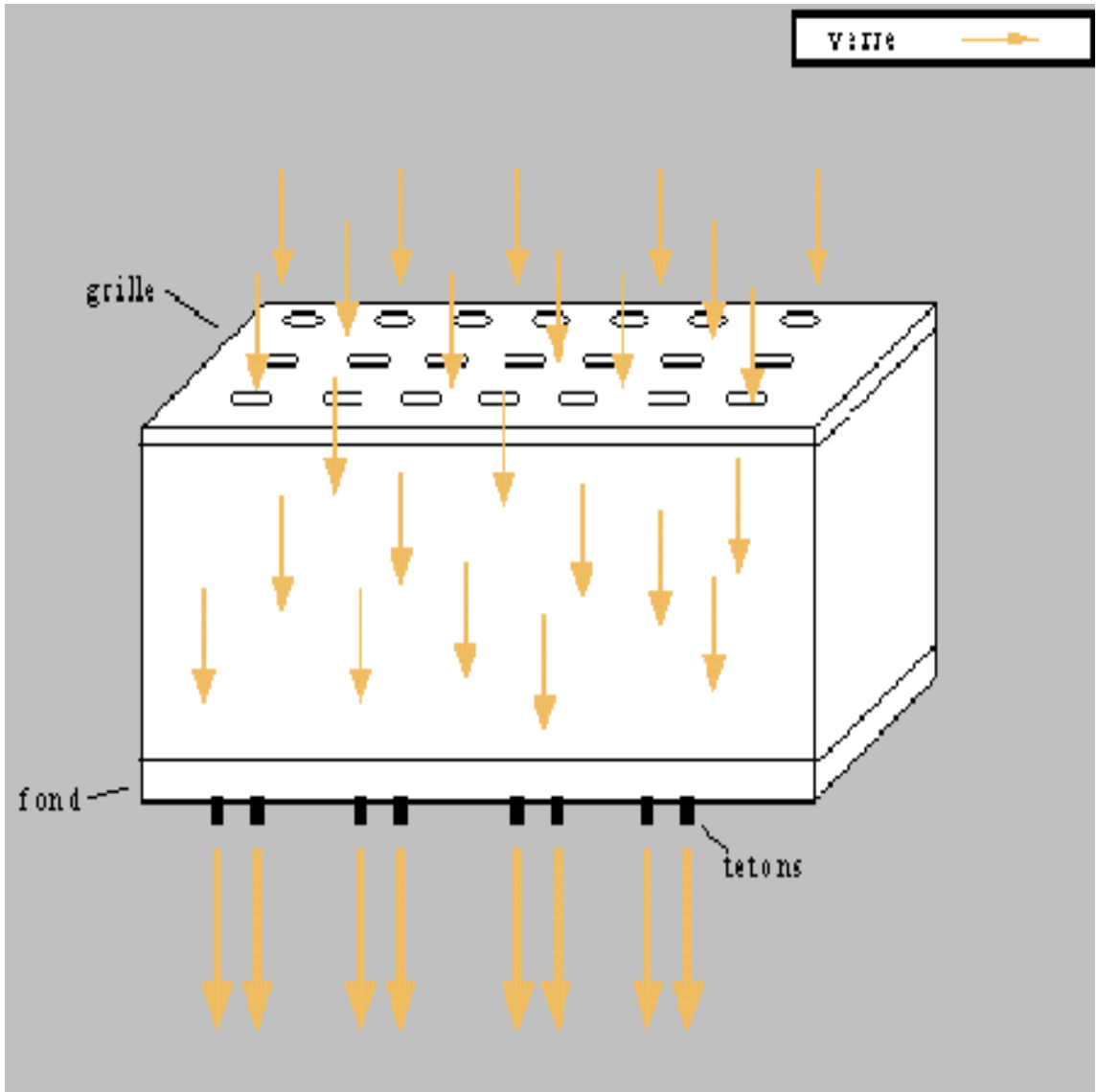Figure A.1: Schema over glass fiber bushing production

Figure A.2: The bushing

37

Appendix B

Bushing 2241US

The massflow for bushing 2241 is 2150 kg/day. The dimension are given in table B.1 and the properties of glass in table B.2. In table 3 are an estimation of the constants needed to calculate the rise time according to equation 3.6.

$Area_{bottom}(m^2)$	$Volume(m^3)$
-	-

Table B.1: Dimensions of bushing 2241US

$c_p(\frac{J}{kgK})$	$\rho(kg/m^3)$
1100	2550

Table B.2: Properties of glass

h $(\frac{W}{m^2K})$	A (m^2)	$c_p(\frac{J}{kgK})$	m (kg)	$\dot{m}(\frac{kg}{s})$
-	-	-	-	-

Table B.3: Estimated physical values for the physics of bushing 2241US

Appendix C

Values used to calculate Power input gain

	$P_0(kW)$	$\Delta P(kW)$	$T_0(^\circ C)$	$\Delta T(^\circ C)$
Zaher	-	-	-	-

Table C.1: Values used to estimate Temperature/Power gain

The values can be found in Annexe 13 for Zaher, the table for bushing 2241US. The corresponding ΔU is - and thermocouple 2 is used for the temperature.

Appendix D

Model structures

The general structure

$$A(q)y(t) = [B(q)/F(q)]u(t - nk) + [C(q)/D(q)]e(t) \qquad \text{(D.1)}$$

Below some of the most commonly used structures are listed.

ARX

A(q)y(t)=B(q)u(t-nk)+e(t)

ARMAX

A(q)y(t)=B(q)u(t-nk)+C(q) e(t)

OE

y(t) = [B(q)/F(q)] u(t-nk) + e(t)

Box-Jenkins

y(t) = [B(q)/F(q)] u(t-nk) + [C(q)/D(q)] e(t)

Appendix E

Passerelle

E.1   Control in the Passerelle

The discrete equation E.1 is used for the control in the S5-95U.

$$U_k = K_d[E_k + TI \sum_{j=0}^{k} E_j] \tag{E.1}$$

Where e_k is the error between temperature and reference and u_k is the action in points. The controller work in points and the measurements are transformed according to equations E.2 and E.3 before use in equation E.1.

$$T_{points} = \frac{1640}{1600}T \tag{E.2}$$

$$U_{points} = \frac{2047}{16}(u_{command} - 4) \tag{E.3}$$

Thus the controller in physical units become equation E.4

$$u_k = k_{points}K_d[e_k + TI \sum_{j=0}^{k} e_j] + 4 \tag{E.4}$$

where $k_{points} = \frac{16}{2047}\frac{1640}{1600}$. Comparing equation G.7 with the parameterizations in equation E.1 gives that the control in the passerelle is indeed a backwards approximation of a continuous time controller. The correspondence between a PID control with parameters T_i and K_c and the S5-95U variables TI and K_d is

$$K_d = K_c \tag{E.5}$$

$$TI = \frac{T_i}{h} \tag{E.6}$$

E.2 Measurement setup in the Passerelle

Black denotes existing material in the passerelle, red are our measuring equipment. The input tension was measured over cables 115-05 and 115-06, and the control current from cables 116-09 and 116-08. For details on the acquisition chain in the passerelle I refer to the documentation.
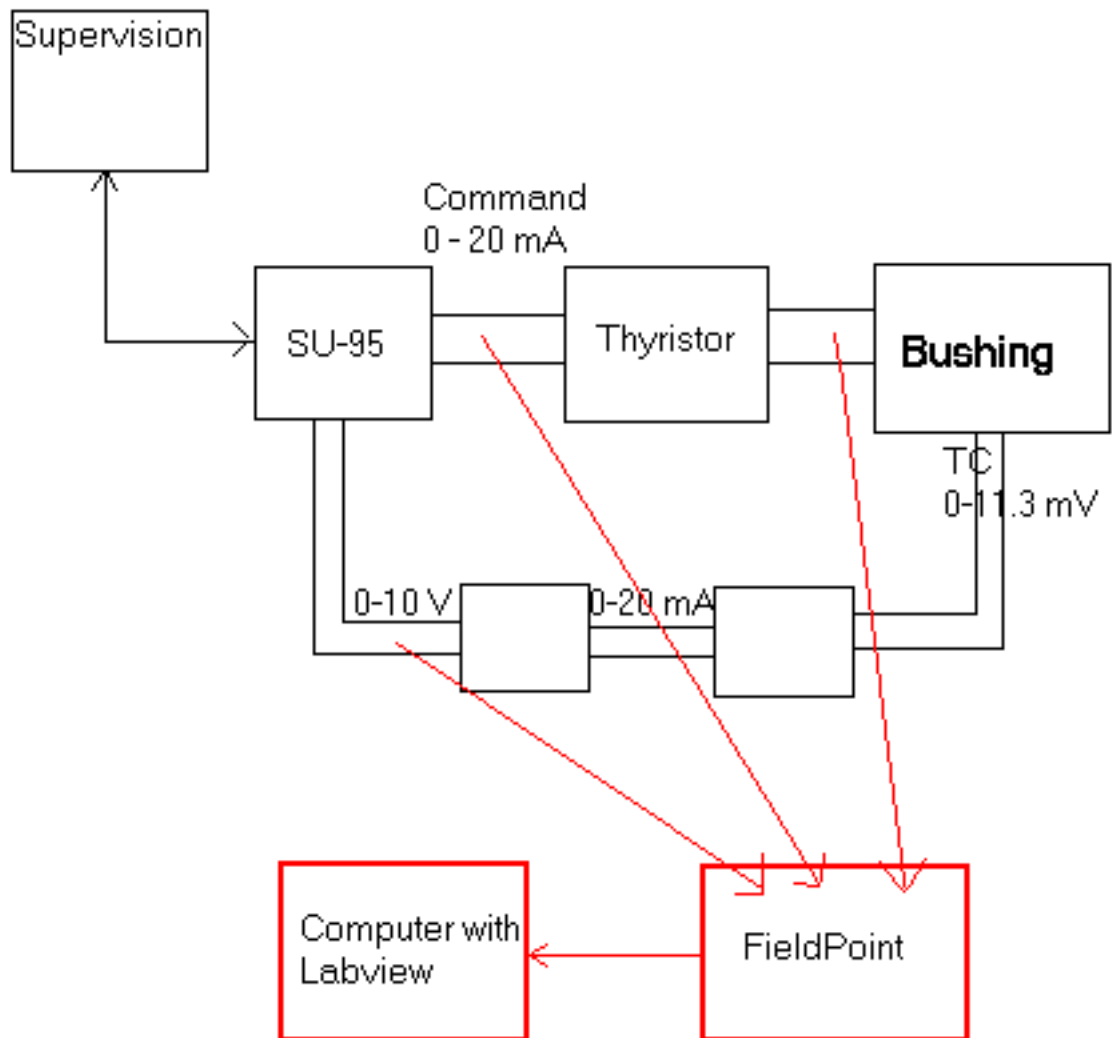
Figure E.1: Measurement locations in the passerelle

Appendix F

Verrerie

F.1 Control in the Verrerie

A TCS6352 is used for the control. This is an discret controller made by Eurotherm, that approximates a PID control. The output is calculated in percentage from the error by equation F.1.

$$OPn = -\frac{100}{XP}(ERn + \frac{T_s}{T_i}ER + \frac{T_d}{T_s}APv) + 50\%$$ (F.1)

T_s (s)	XP	T_i (s)	T_d (s)
-	-	-	-

Table F.1: Values used in the TCS-6352 for bushing unit 75

As T_d is zero when can compare this with the discretization of the PID in annexe G. This gives $K = \frac{100}{XP} = -$ and $T_i = T_{iTCS} = -$

F.2 Measurement setup in the Verrerie

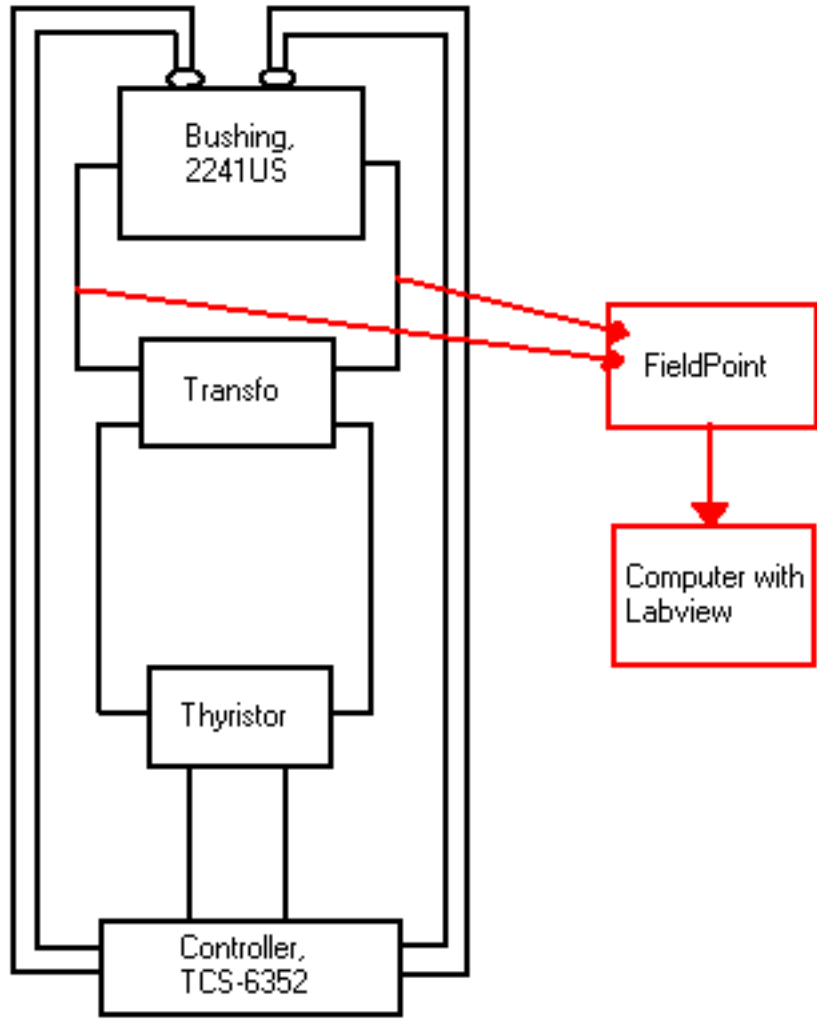Black denotes existing material in the Verrerie, red are our measuring equipment.

Figure F.1: Measurement locations in the Verrerie

Appendix G

The PID controller

A standard form for the PID controller is equation G.1 even though there exists many variations on how to write this.

$$u(t) = K[e(t) + \frac{1}{T_i} \int_{s=0}^{t} e(s)\delta s + T_d \frac{\delta e(t)}{\delta t}] \tag{G.1}$$

This equation can be decomposed into three parts. A proportional, integral and derivative part.

$$P(t) = Ke(t) \tag{G.2}$$

$$I(t) = \frac{K}{T_i} \int_{s=0}^{t} e(s)\delta s \tag{G.3}$$

$$D(t) = KT_d \frac{\delta e(t)}{\delta t} \tag{G.4}$$

As a neither a true derivative nor a true integral can be implemented on a computer an approximation has to be made if computers are to be used. Once more several approxiamtion methods exist. The proportional part does not need to be approximated and can be taken as it is.

$$P(t_k) = Ke(t_k) \tag{G.5}$$

Approximating the integral part with a backwards approximation gives equation G.6

$$I(t_{k+1}) = I(t_k) + \frac{Kh}{T_i} e(t_{k+1}) \tag{G.6}$$

where h denotes sampling time. Using equations G.5 and G.6 gives an approximation of a PI-controller.

$$u(t_k) = K[e(t_k) + \frac{h}{T_i} \sum_{j=0}^{k} e(t_j)] \tag{G.7}$$

Appendix H

Matlab files to obtain the models

In this annexe some of the matlab .m files created for the identification are listed.

1. **Prep.m** Loads the data, selects work sequences, remove averages, etc

2. **CalcDI.m** Calculation of models etc.

3. **Graphs.m** Various plots useful for validation

Table H.1: List of matlab files written for the identification

H.1   prep.m

```
% Load the data from final experiment, FP3 and FP1, into Matlab
load essaiFP3;

% Extract the variables.
u=essaiFP3(:,3);T=essaiFP3(:,4);r=essaiFP3(:,5);
U=essaiFP3(:,6);I=essaiFP3(:,7);

%Calculate electrical Power (in kW)
P = U.*I/1000;
```

```
% Get average levels
u30 = mean(u); T30 = mean(T);r30 = mean(r);P30 = mean(P);

%Choix of work data
u=u(500:4850);T=T(500:4850);r=r(500:4850);U=U(500:4850);I=I(500:4850);
P=P(500:4850);

% Set initial value to zero
T3c = T-T(1)*ones(length(T),1); u3c = u-u(1)*ones(length(u),1);
r3c = r-r(1)*ones(length(r),1); P3c = P-P(1)*ones(length(P),1);

% The estimation functions take z=[y,u] as workdata
u2T3=[T3c,u3c]; r2T3=[T3c,r3c]; r2u3=[u3c,r3c]; P2T3=[T3c,P3c];

% Part FP1
load essaiFP1; u=essaiFP1(:,3);T=essaiFP1(:,4);r=essaiFP1(:,5);
U=essaiFP1(:,6);I=essaiFP1(:,7); P = U.*I/1000; u10 = mean(u); T10
= mean(T);r10 = mean(r);P10 = mean(P);
u=u(1:2000);T=T(1:2000);r=r(1:2000);U=U(1:2000);I=I(1:2000);P=P(1:2000);
T1c = T-T(1)*ones(length(T),1);u1c = u-u(1)*ones(length(u),1);r1c
= r-r(1)*ones(length(r),1); P1c = P-P(1)*ones(length(P),1);
u2T1=[T1c,u1c]; r2T1=[T1c,r1c]; r2u1=[u1c,r1c]; P2T1=[T1c,P1c];

% Prefiltering
u2T3f = idfilt(u2T3,5,0.047746); r2T3f = idfilt(r2T3,5,0.047746);
P2T3f = idfilt(P2T3,5,0.047746); u2T1f = idfilt(u2T1,5,0.047746);
r2T1f = idfilt(r2T1,5,0.047746); P2T1f = idfilt(P2T1,5,0.047746);

clear essaiFP1 essaiFP3 u T U I P r;
```

H.2   CalcDI.m

```
% Calculation of model between control current and temperature
thDI1 = arx(u2T3f,[3 3 0],[],1);
```

```
% Physics
thDIP = arx(P2T3f,[3 3 0],[],1);
```

H.3 Graphs.m

```
function Graphs(Z,th);
% Graphs(Z,th);
% Z = [y,u] validationdata
% th : model
% Graphs of simulation, prediction, residuals and steprespons


% Simulering av utsignal
figure compare(Z,th); ylabel('Temperature [C]'); xlabel('Time
[s]'); LEGEND('Model output','Measured output'); grid on; xmin =
0; xmax = 1800;ymin = -10;ymax =10 ; axis([xmin xmax ymin ymax]);
print -depsc SimuDI


% Prediction av utsignal
figure; yp = predict(Z,th,15); plot(yp); hold on;
plot(Z(:,1),'k'); hold off; ylabel('Temperature [C]');
xlabel('Time [s]'); LEGEND('Predicted output','Measured output');
grid on; xmin = 0; xmax = 1800;ymin = -10;ymax =10 ; axis([xmin
xmax ymin ymax]); print -depsc PredDI

% Berakning av residual
figure e = resid(Z,th); print -depsc ResidDI

% Stepresponse and varians
step1 = [zeros(3,1); ones(900,1)]; [y, ysd] = idsim(step1,th);
figure plot(y);hold on;plot(y+ysd,':');plot(y-ysd,':'); hold off;
ylabel('Temperature [C]'); xlabel('Time [s]'); print -depsc
StepDI
```

Appendix I

Bushing 3, Passerelle

Series	P_{mean} (kW)	u_0 (mA)	$T_{mean}(°C)$	$r_0(°C)$	$\Delta r(°C)$
FP3	-	-	-	-	-
FP1	-	-	-	-	-

Table I.1: Operating values in the Passerelle for the identification data

I.1 Direct Identification

The direct method gave equally good results as the three step method. Thus all the result here comes from the direct identification. Both the power and command current models uses an ARX structure, see equation I.1. Sd denotes standard deviation. The samplig time is 1s.

$$A(q)y(t) = B(q)u(t - nk) + e(t) \tag{I.1}$$

Coefficient	a_1	a_2	a_3	b_1	b_2	b_3	n_k
Value	-2.9753	2.9528	-0.9775	0.0898	-0.1779	0.0882	0
Sd	0.0017	0.0034	0.0017	0.0016	0.0032	0.0016	0

Table I.2: Temperature / Command current

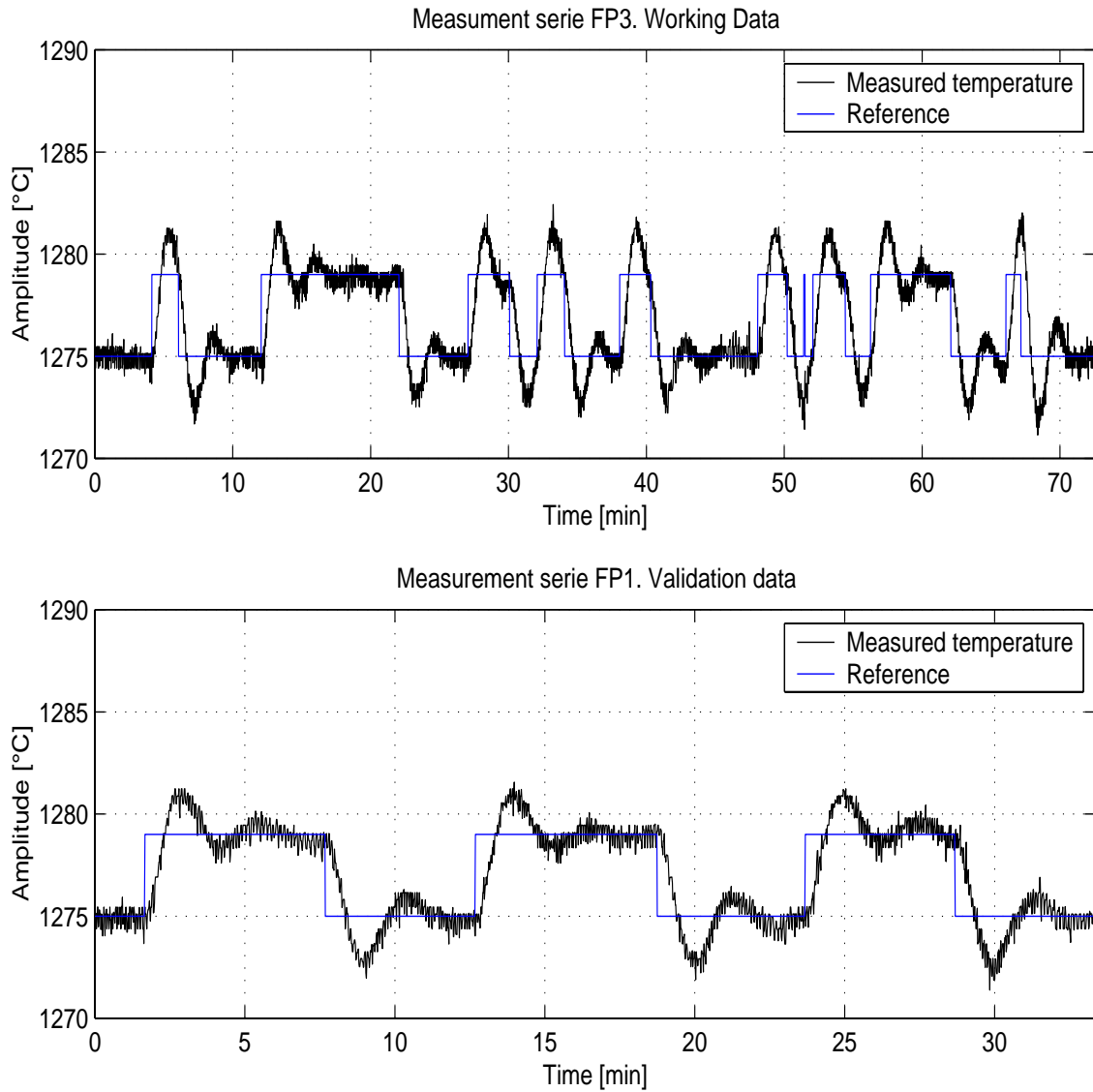| Coefficient	a_1	a_2	a_3	b_1	b_2	b_3	n_k
Value	-2.9705	2.9431	-0.9725	0.0738	-0.1462	0.0725	0
Sd	0.0017	0.0033	0.0016	0.0012	0.0024	0.0012	0

Table I.3: Temperature / Power

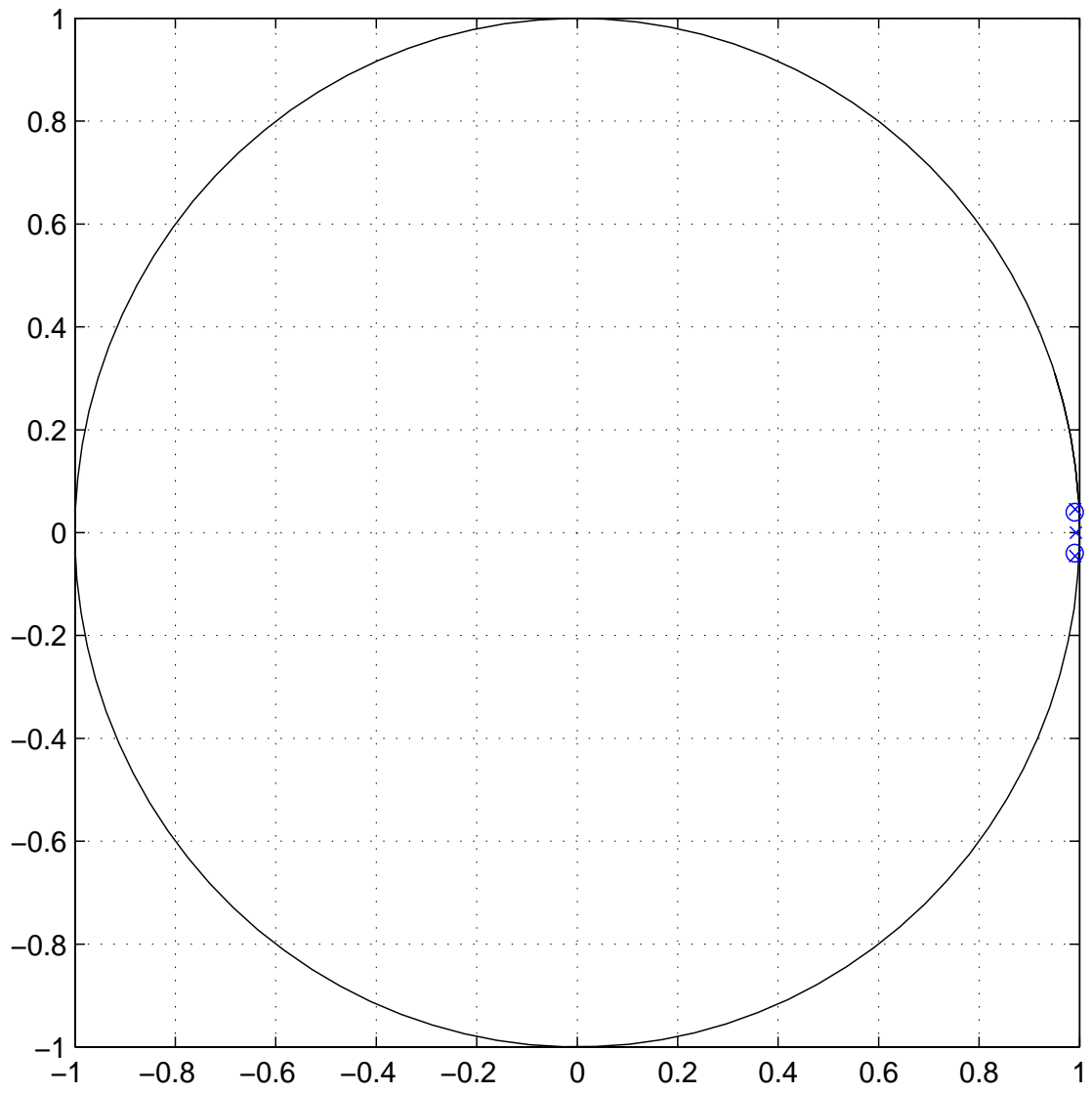Figure I.1: Measured temperature FP3 and FP1 series
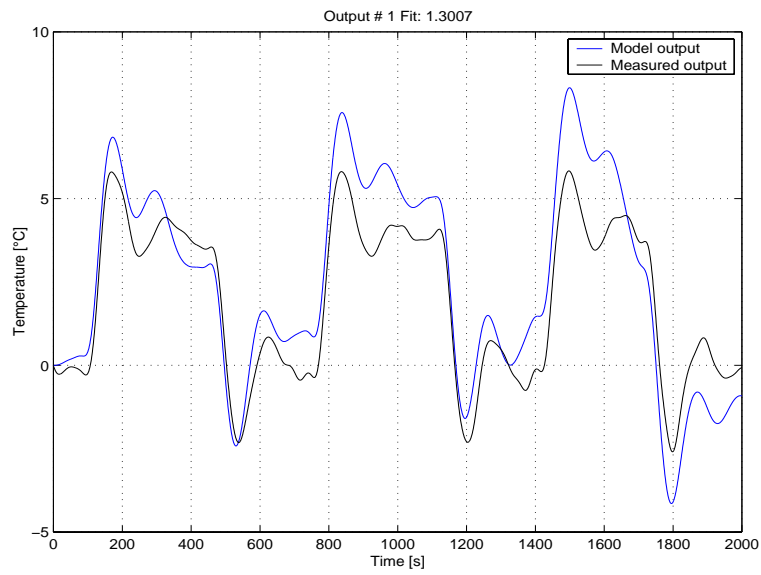
52

Figure I.2: Zero-poles plot

53

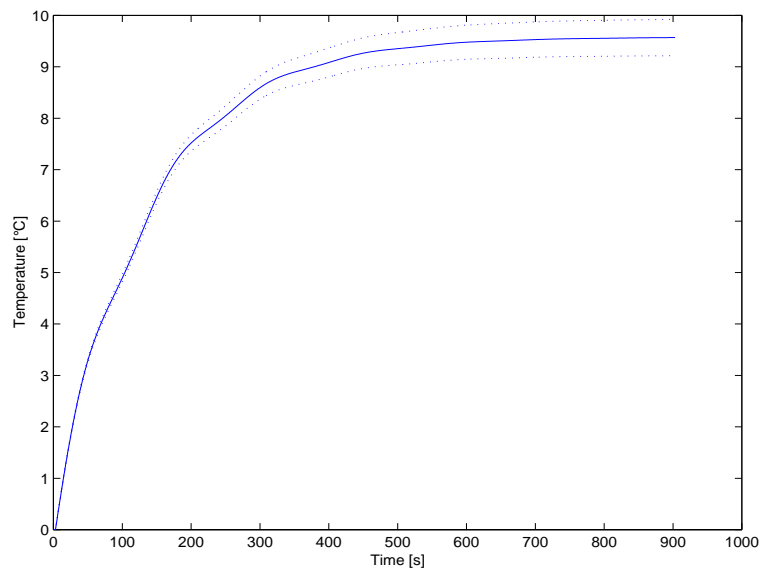Figure I.3: Simulated and measured output, Input command current
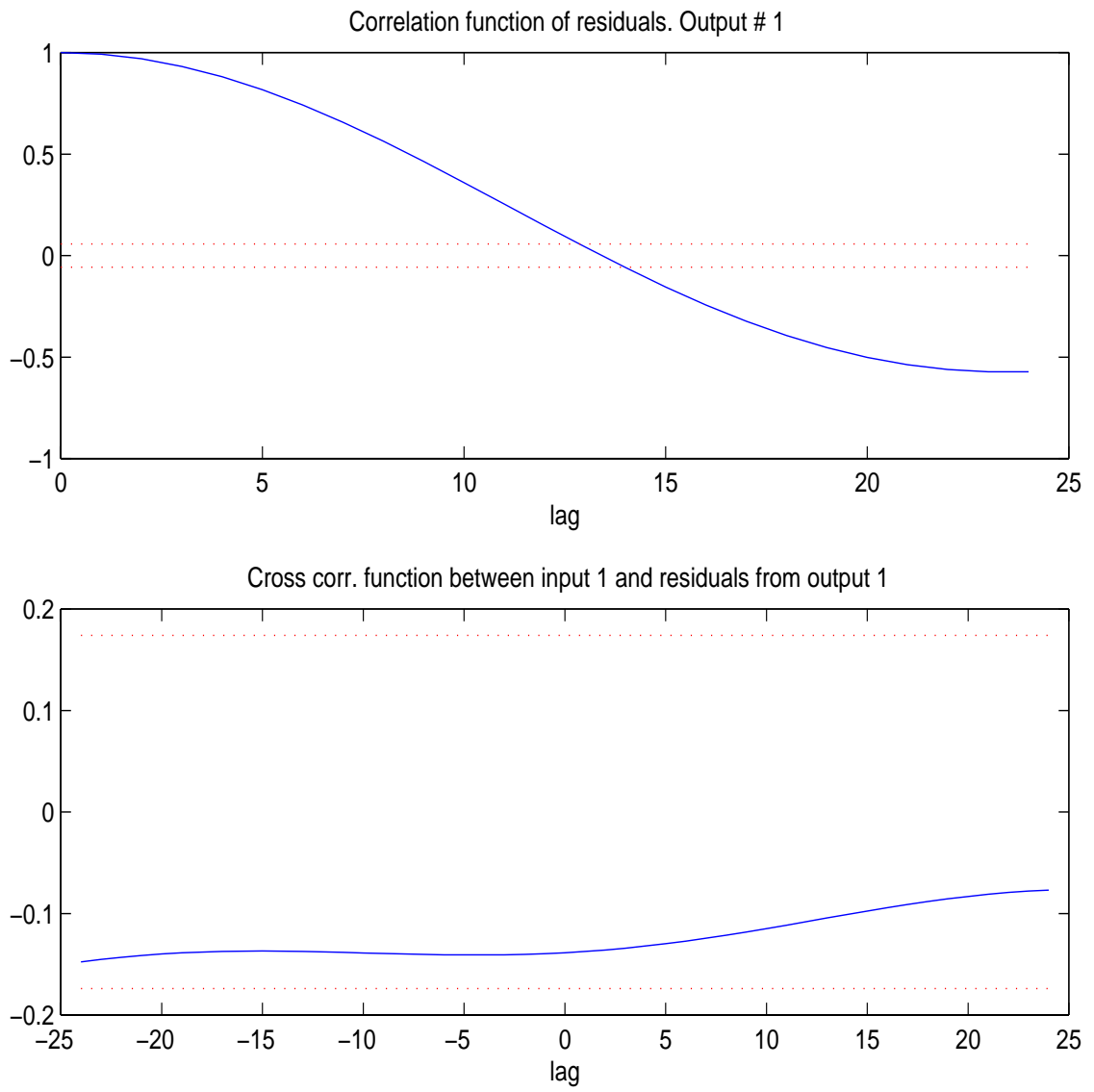

Figure I.4: Step response, Input command current
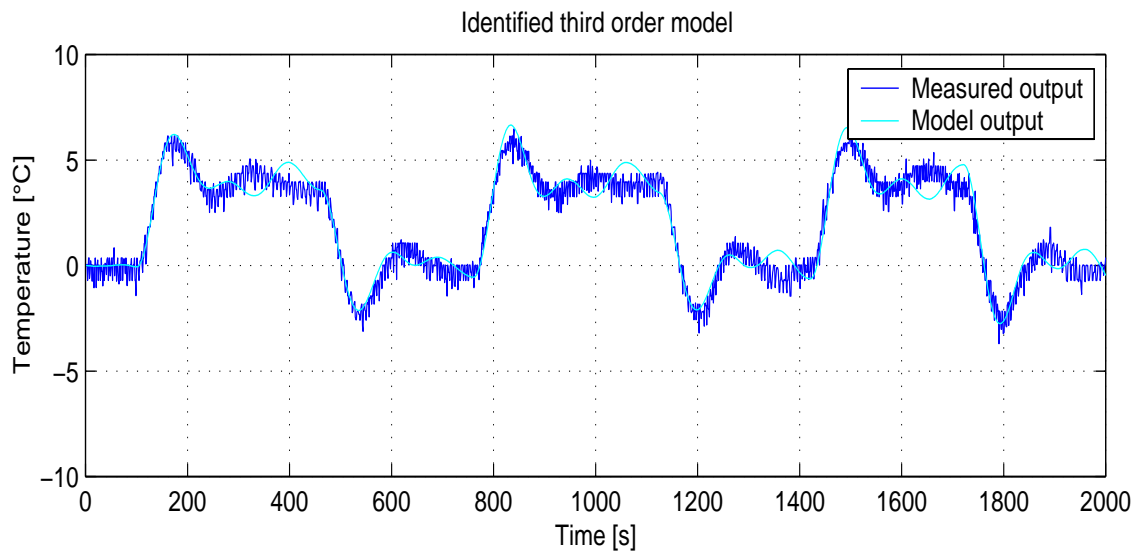
54

Figure I.5: Residuals, Input command current
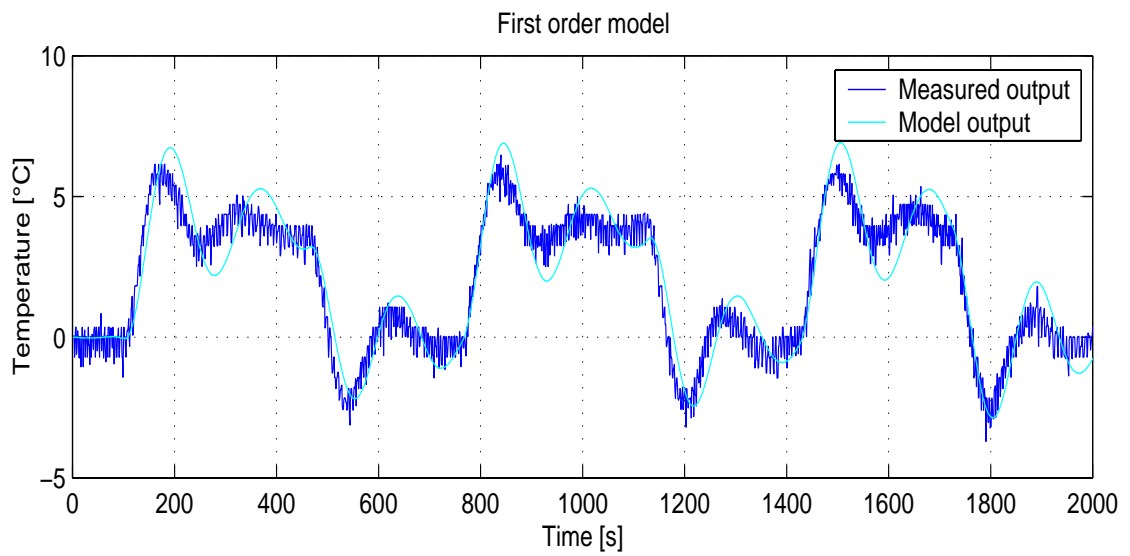
Figure I.6: Closed-loop simulation, Passerelle

Appendix J

Bushing 2241US, Verrerie

The identification in the verrerie was made between the OP and temperature. These values were all taken from the TCS-6352 with Intouch. In addition the gain between power and temperature has been estimated from the power measurement with Field Point and the Temperature. The sampling time is 1s.

Series	Pp_{mean} (kW)	Ps_{mean} (kW)	u_0 (OP)	$T_{mean}(°C)$	$r_0(°C)$	$\Delta r(°C)$
Work, Verr3	-	-	-	-	-	-
Validation, Verr2	-	-	-	-	-	-

Table J.1: Operating values in the Verrerie

J.1 Three step method

Both the power and command current models uses an OE structure, see equation J.1. Sd denotes standard deviation.

$$y(t) = [B(q)/F(q)]u(t - nk) + e(t) \qquad \text{(J.1)}$$

Coefficient	f_1	f_2	f_3	b_1	b_2	b_3	n_k
Value	-2.7100	2.4474	-0.7372	0.0579	-0.0970	0.0400	0
Sd	0.0055	0.0104	0.0048	0.0004	0.0011	0.0007	0

Table J.2: Temperature / Command current

Coefficient	f_1	f_2	f_3	b_1	b_2	b_3	n_k
Value	-2.8768	2.7611	-0.8842	0.2166	-0.4012	0.1911	0
Sd	0.0009	0.0016	0.0008	0.0007	0.0015	0.0008	0

Table J.3: Temperature / Power
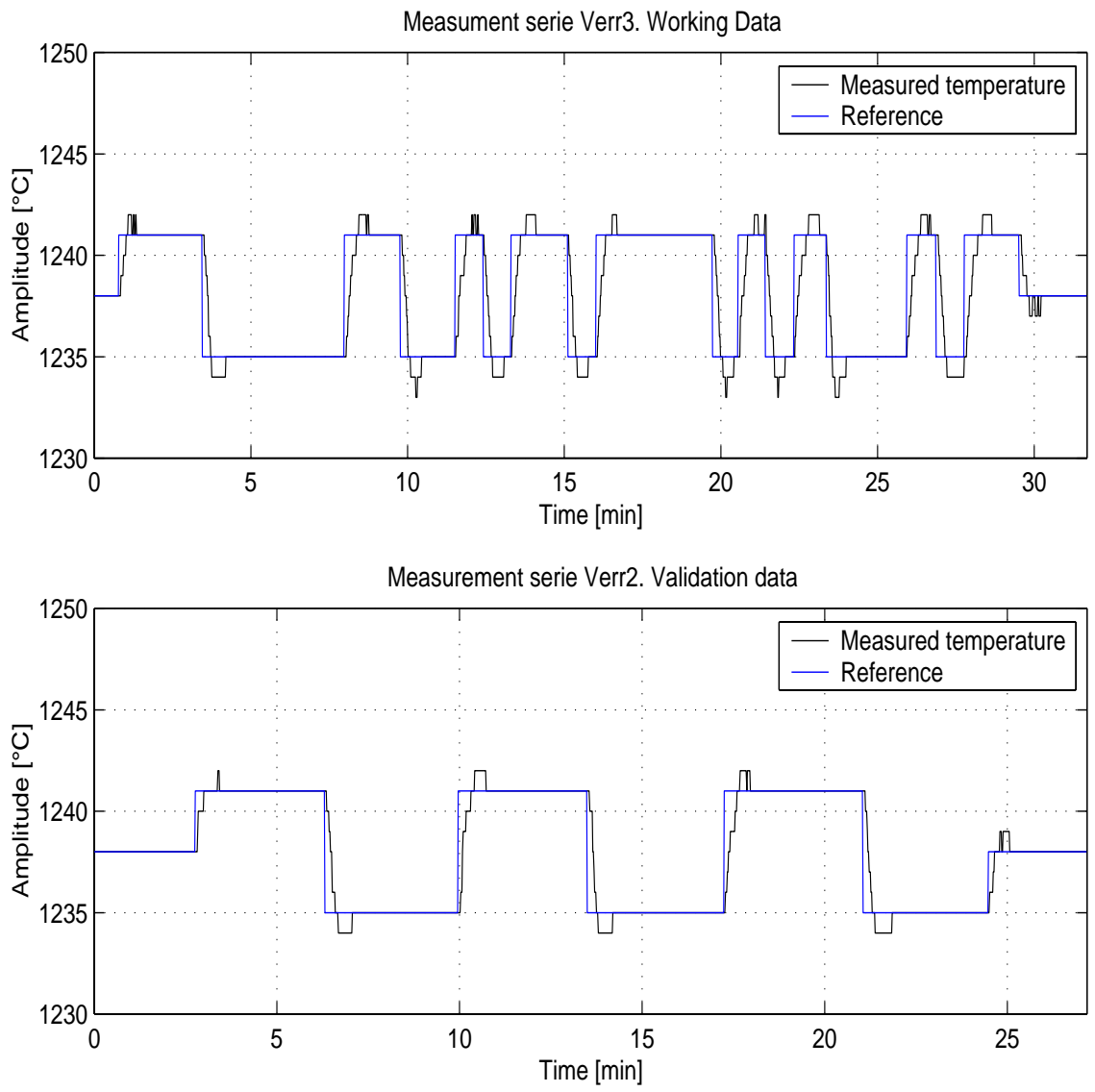
Figure J.1: Measured temperature Verr3 and Verr2 series
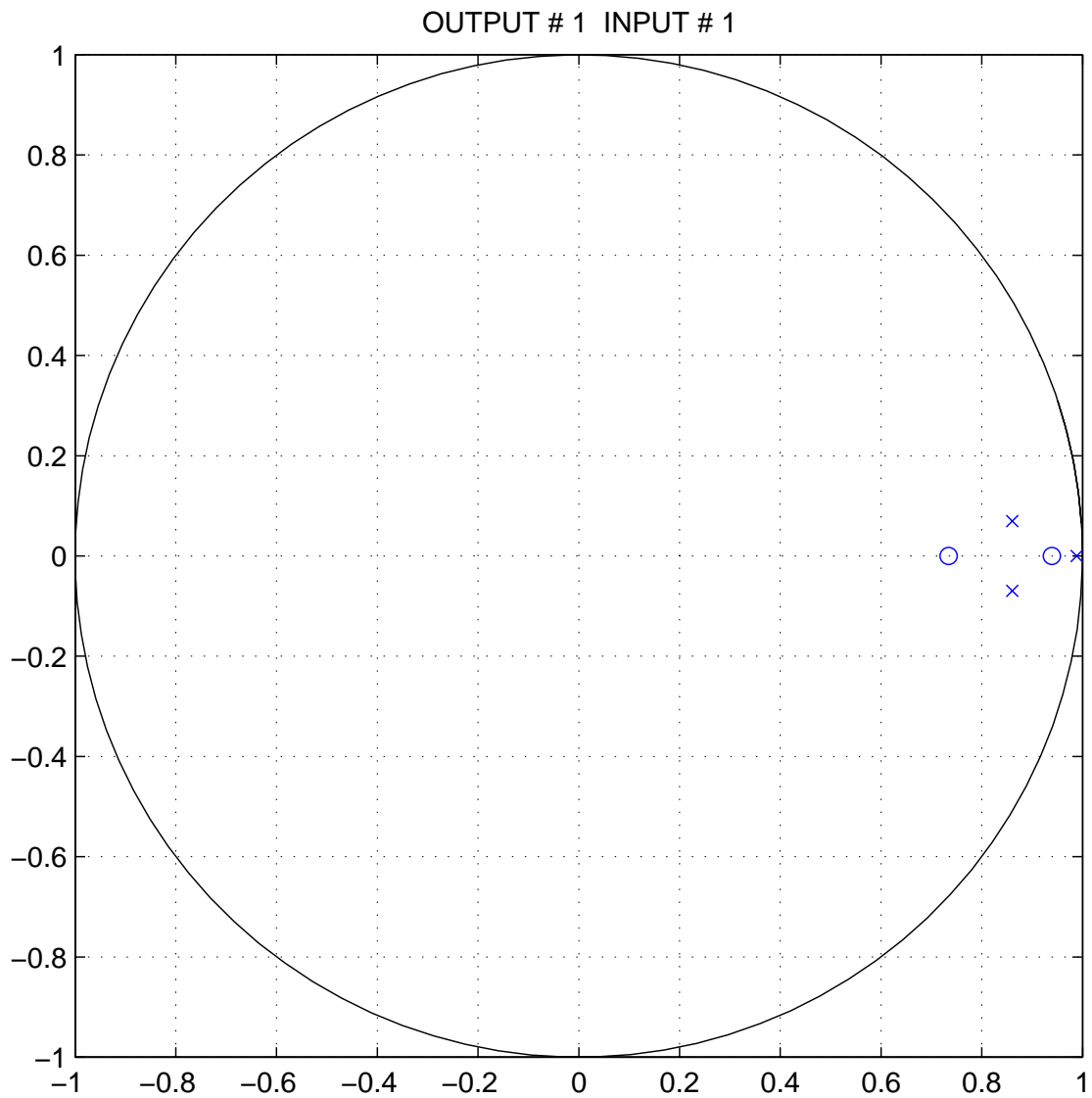
59

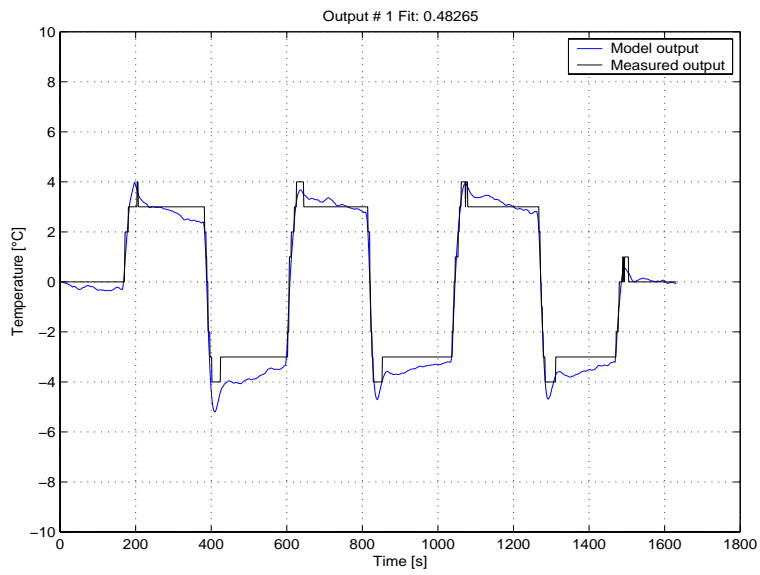Figure J.2: Zero-Pole plot

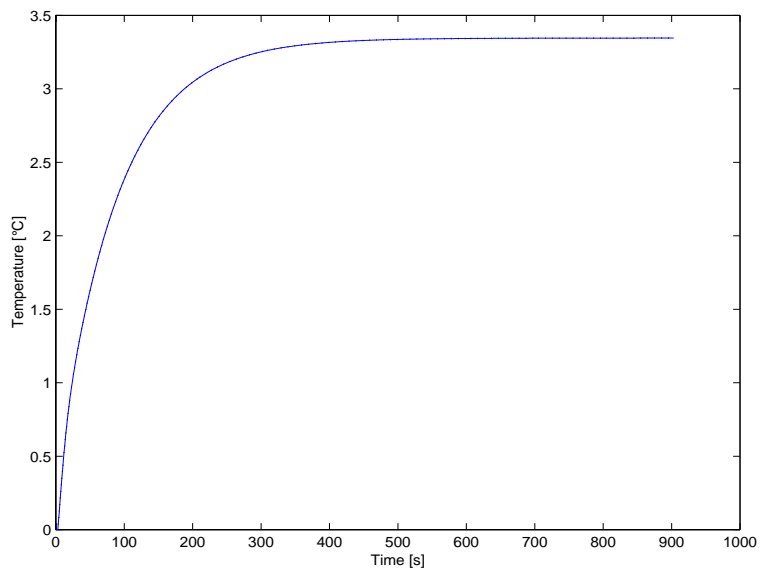Figure J.3: Open loop simulated and measured output, Input OP
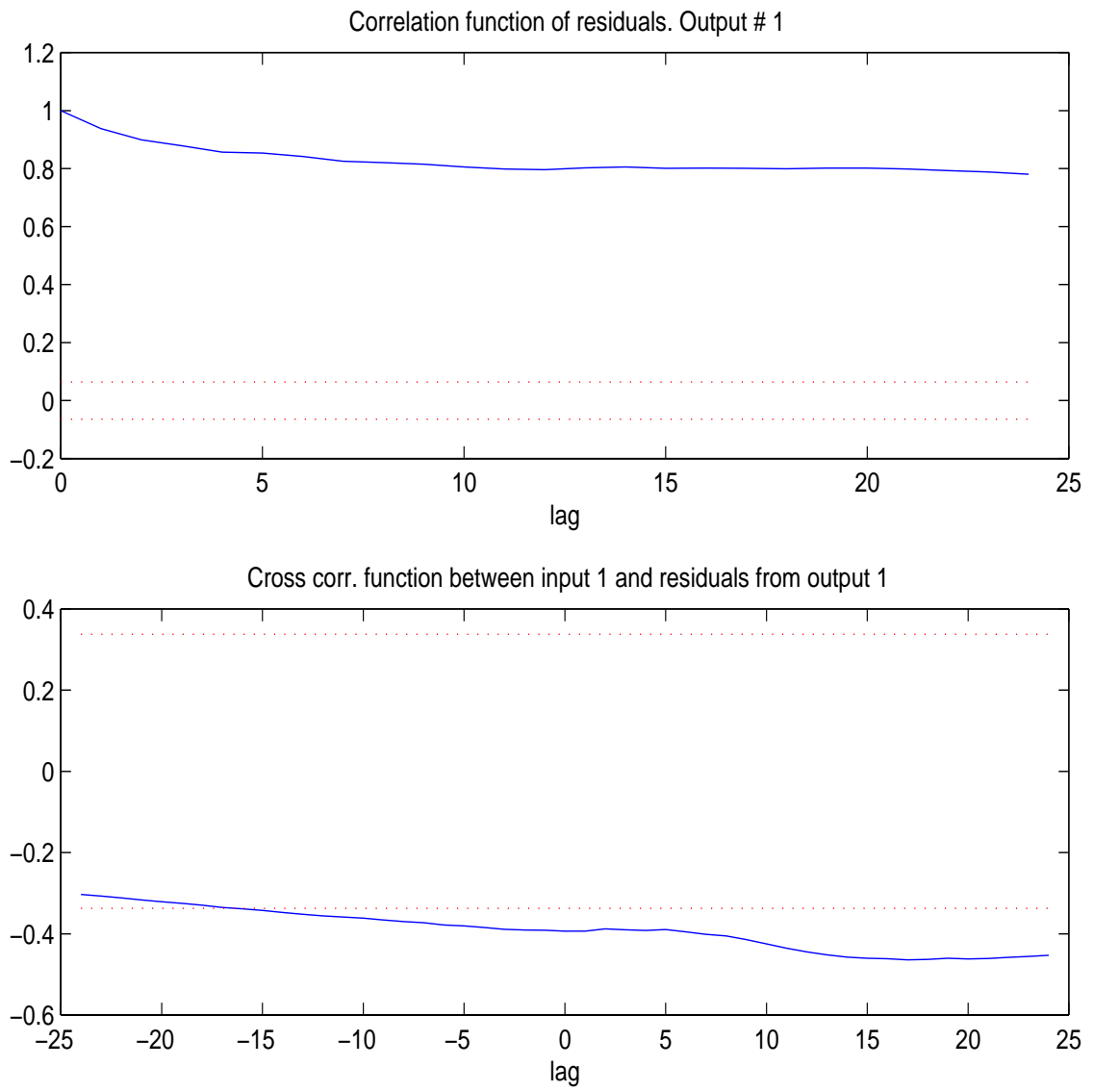

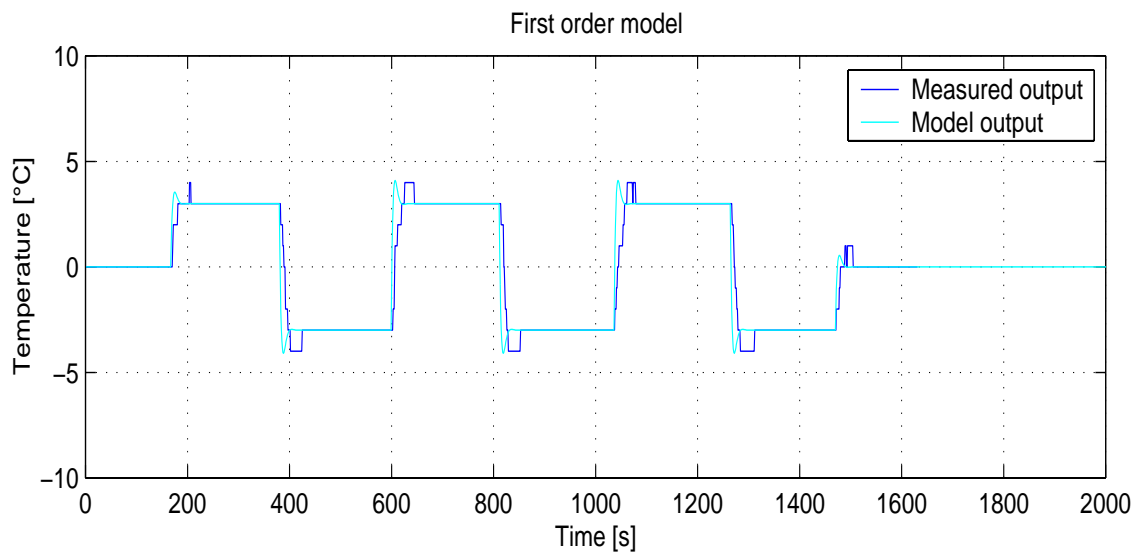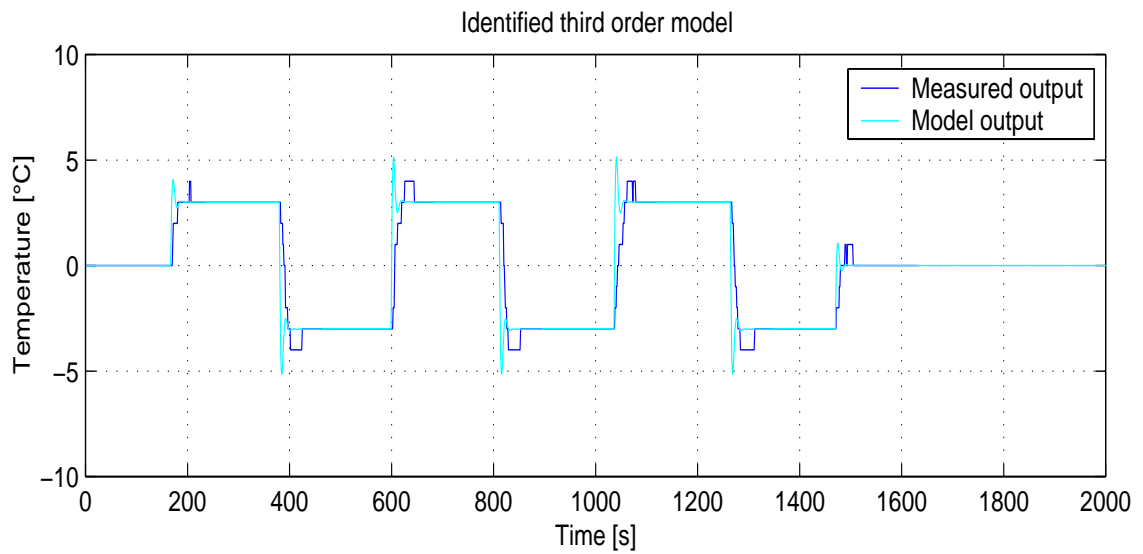Figure J.4: Step response, Input OP

61

Figure J.5: Residuals, Input OP

Figure J.6: Closed-loop simulation, Verrerie

Appendix K

Comparison Labview and Fieldpoint vs PLC S5-95U

For the DAQ part two things differed between the two systems. The resolution of the input and output and the stability. Table K.1 shows the differences.

	Input resolution	Output resolution	Optically separated inputs
SU-95	10 bits (1.5°C)	12bits	No
FieldPoint	16 bits (0.02°C)	16 bits	Yes

Table K.1: Comparison between S5-95U and FieldPoint

In terms of hardware Fieldpoint is clearly preferable to the SU-95. As the acquisition part of the Labview program was already written a PID control could quickly be implemented. As Labview uses a high level programing language changes and more advanced programs useful fore the experiments could be implemented. Se table **??** for a list of the advantages.

1. Significantly lower noise levels thanks to optically separated input channels.

2. Greater resolution, from 10 bits to 16 bits or 1.5°C to 0.02 ° C, thus 64 times better!

3. Complete control of all aspects of the control loop. The control equation used, sampling period, all values used for the control.

4. Data synchronisation. All the data is stored on one computer instead of on two.

5. A better closed loop performance is obtained.

6. Easy implementation of improvements

Table K.2: Advantages of Labview control

Bibliography

[Ljung] L., Ljung *System Identifcation : Theory for the user* Prentice Hall, Inc., 1987, Englewood cliffs, New Jersey

[Zaher] N. Zaher *Etude des filières 2242 et 4264 pour l'amlioration de la rgulation.*1999, Rapport de stage VI/UTC

[Pillon] T. Pillon *Optimisation thermique et aeraulique d'une position de fibrage* 1993, Rapport de stage VF/E.S.I.-GTI de Pau

[Hof] P. Van den Hof *Closed-Loop issues in system identification, Interaction entre l'identification et la command*1998, Ecole d'été d'automatique, LAG, Grenoble.

[Young] Hugh D. Young, Roger A. Freedman *University Physics, 9th ed.* Addison-Wesley publishing company, Inc., 1996,

[Åstrom] Karl J. Åstrom *Reglerteknik*Almqvist & Wiksell, 1985, Goteborg

[Wittenmark] Karl J. Åstrom, Bjorn Wittenmark *Computer-Controlled systems, Theory and design* Prentice Hall, Inc., New Jersey.

[Chebassier] Joel Chebassier *Méthodologies pour la conception d'un systéme de commande par calculateur*1998, Ecole d'été d'automatique, LAG, Grenoble.